

# 1 Supplementary Information

## 2 1. Two-stage model description

3  
4 The model of marine-terminating glacier evolution used in this study is described in detail in  
5 Robel et al. (2018). Here, we given an abbreviated description of the model, and the choices  
6 made for various model components which are specific to this study.

7  
8 The model consists of two coupled ordinary differential equations, which describe the evolution  
9 of spatially averaged ice thickness in the glacier interior ( $h$ ) and grounding line position ( $L$ )

$$10 \quad \frac{dH}{dt} = P - \frac{Q_g}{L} - \frac{H}{h_g L} (Q - Q_g) \quad (1)$$

$$11 \quad \frac{dL}{dt} = \frac{1}{h_g} (Q - Q_g) \quad (2)$$

12 Where  $P$  is the spatially averaged surface mass balance,  $Q_g$  is the ice flux through the grounding  
13 line (see more below),  $Q$  is the ice flux in the glacier interior (also see below), and  $h_g$  is the ice  
14 thickness at the grounding line. The first equation tracks the mass flow through the marine-  
15 terminating glacier interior and the corresponding evolution of the glacier thickness. The second  
16 equation tracks the moving boundary (the grounding line) that controls the magnitude of ice flux  
17 out of the glacier.

18  
19 The grounding line is the location where ice is sufficiently thin to float in seawater, and so the  
20 grounding-line ice thickness is exactly at hydrostatic equilibrium with the local water depth

$$21 \quad h_g = -\lambda b(L) \quad (3)$$

22 where  $\lambda = \rho_w/\rho_i$  is the ratio between the densities of seawater and glacial ice, and  $b(L)$  is the  
23 depth of the bed below sea level at the grounding line.

24  
25 When, in the glacier interior, there is a leading-order balance between gravitational driving stress  
26 and basal shear stress set by a Weertman-style friction law ( $Cu^{\frac{1}{n}}$ ), the ice flux is given by

$$27 \quad Q = \left(\frac{\rho_i g}{C}\right)^n \frac{H^{2n+1}}{L^n} \quad (4)$$

28 where  $g$  is the acceleration due to gravity,  $C$  is the basal friction coefficient, and  $n$  is the flow law  
29 exponent for ice.

30  
31 Ice flux through the grounding line or terminus ( $Q_g$ ) is generally thought to be a function of the  
32 local ice thickness ( $h_g$ )

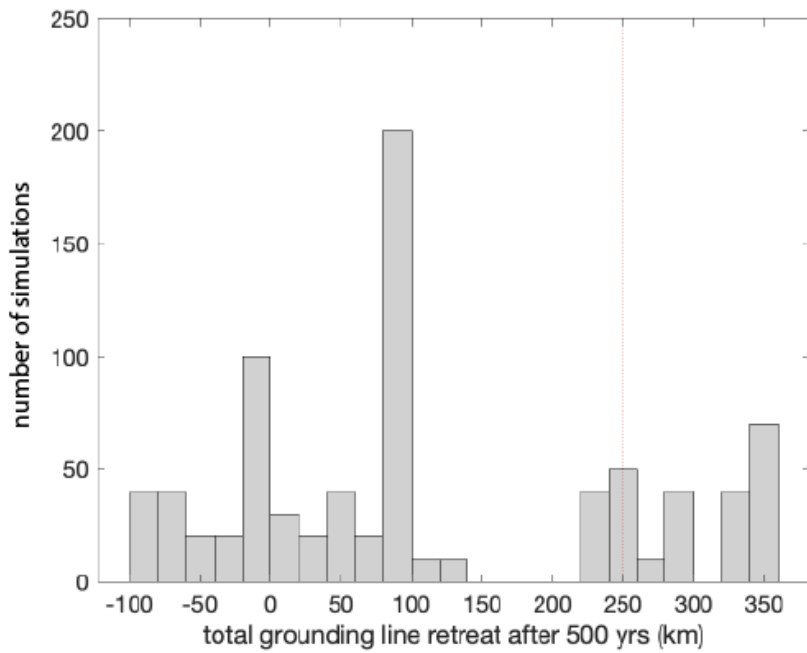
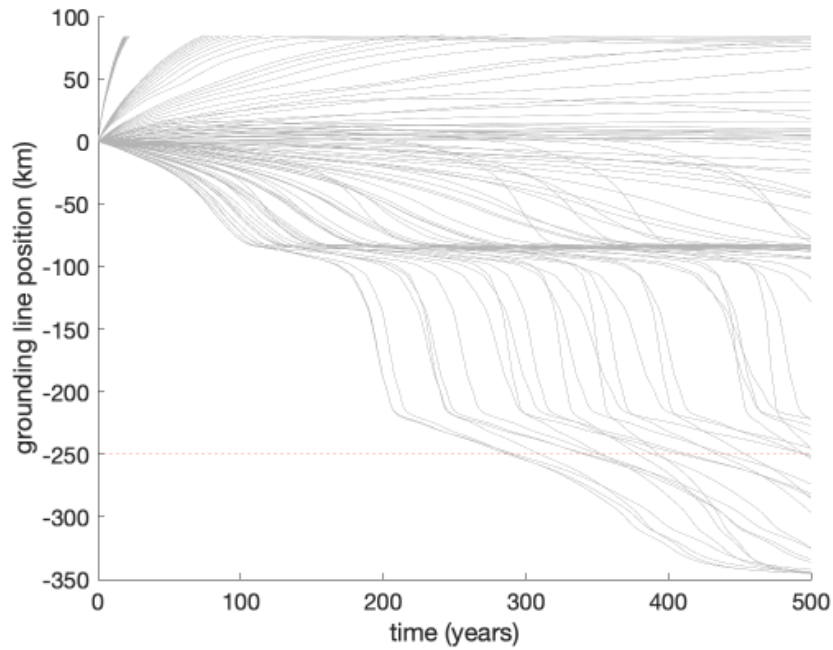
$$33 \quad Q_g = \Omega h_g^\beta \quad (5)$$

34 where  $\beta$  is an exponent that can be derived from various mathematical approaches (Lingle 1984,  
35 Schoof 2007, Hindmarsh 2012, Tsai et al. 2015, Schoof et al. 2017, Haseloff et al. 2018), or  
36 estimated empirically for tidewater glacier termini (Pelto & Warren 1991).  $\Omega$  is a scalar  
37 parameter which incorporates the various factors (besides ice thickness) that can influence ice  
38 flux in the grounding zone or near the terminus. In this study, we pick  $\Omega$  and  $\beta$  given by the  
39 asymptotic analysis of Schoof 2007, where

$$40 \quad \beta = \frac{n^2+3n+1}{n+1} \quad (6)$$

$$41 \quad \Omega = [A_g(\rho_i g)^{n+1}(\theta(1-\lambda^{-1}))^n(4^n C)^{-1}]^{\frac{n}{n+1}} \quad (7)$$

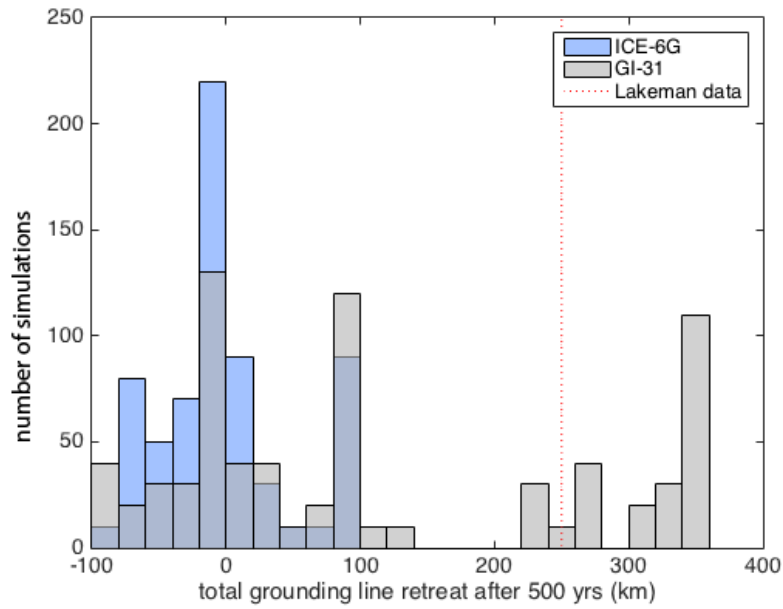
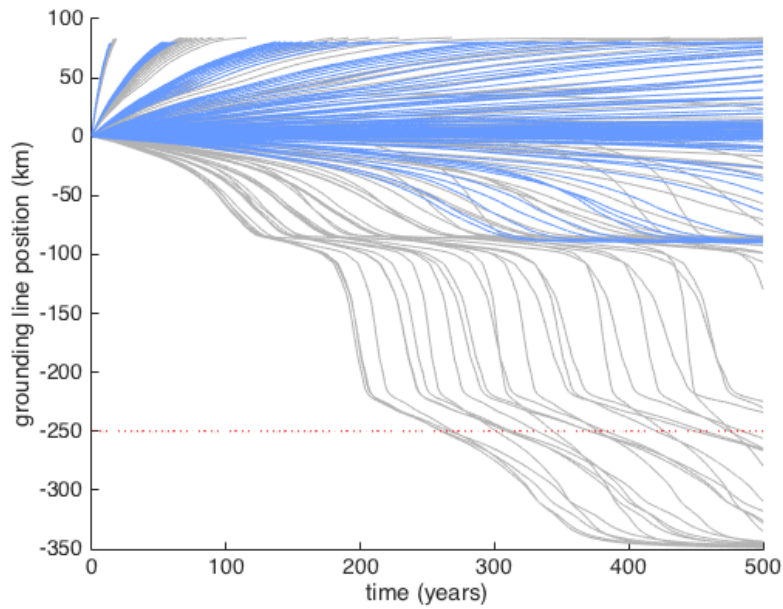
42 and  $\theta$  is a buttressing parameter which parameterizes the effect of ice shelf buttressing, where  
43  $\theta = 0$  indicates full buttressing and  $\theta = 1$  indicates no buttressing. Robel et al. (2018)  
44 demonstrates how this model reproduces the most important aspects of spatially-extended  
45 models of marine-terminating glacier evolution.  
46



47

48

49 Appendix Figure 1 | Simulations that repeat the analysis shown in the main text (Figure 4) using paleotopography  
 50 associated with GI-31 at 12.5 ka (see text for details). Grounding line position (relative to the initial position) is  
 51 calculated from the marine-terminating glacier model using the GI-31 (gray) paleotopography. The dotted red line is  
 52 the total grounding line retreat of the Amundsen Ice Stream reported by Lakeman et al. (2018). In these simulations  
 53 190/1000 produced over 250 km of grounding line retreat within 500 years  
 54



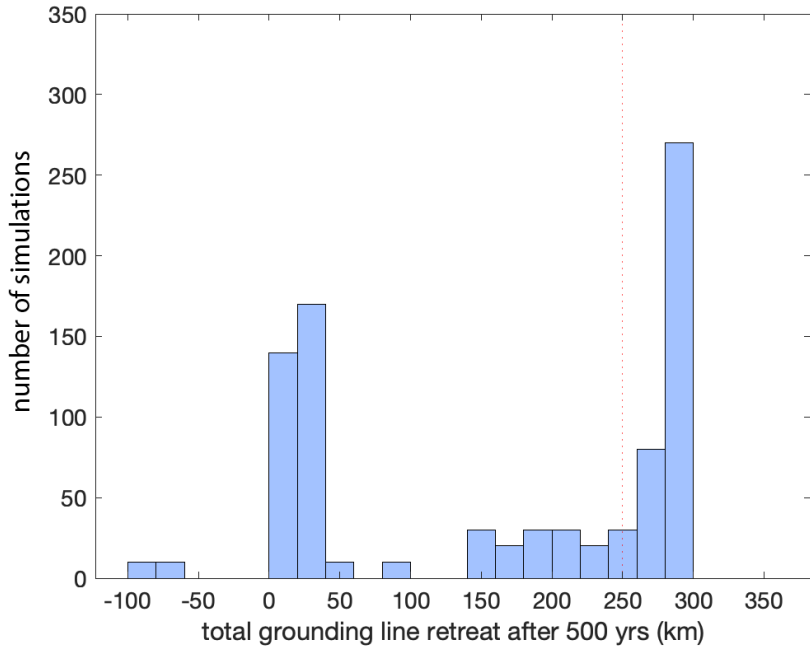
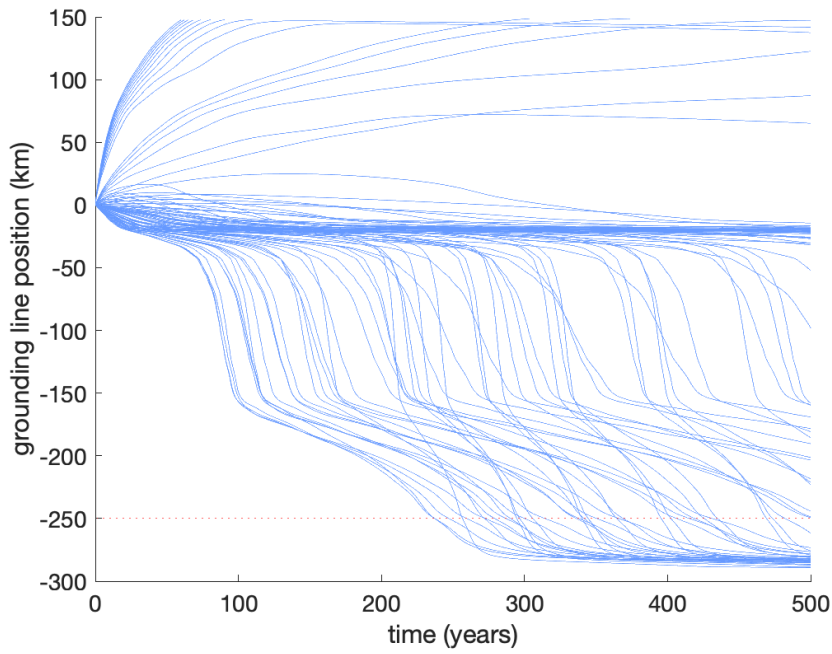
56

57 Appendix Figure 2| Simulations that repeat those shown in the main text (Figures 4, 5) using an alternate Earth  
58 model alternate Earth model characterized by a lithospheric thickness of 48 km, and an upper and lower mantle  
59 viscosities of  $5 \times 10^{20}$  Pa s and  $5 \times 10^{21}$  Pa s, respectively.

60

61

62



63

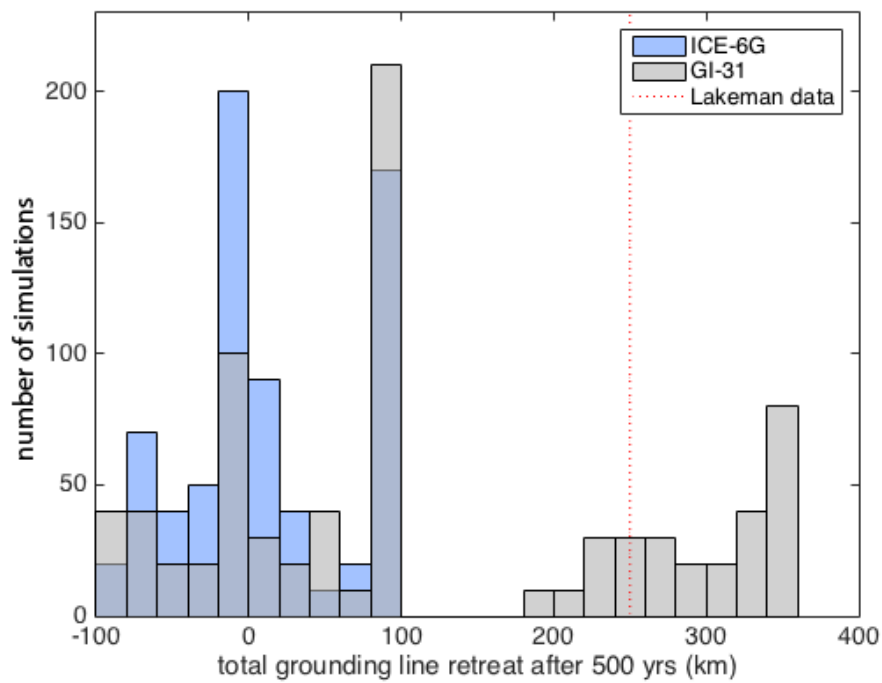
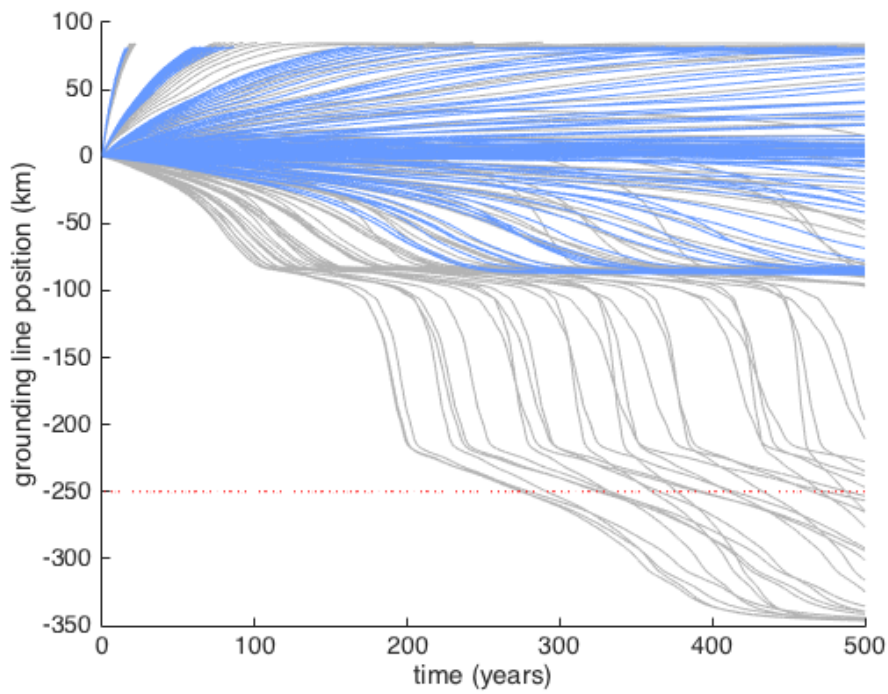
64

65 Appendix Figure 3 | Simulations that repeat those shown in the main text (Figures 4, 5) using an ice profile and

66 paleotopography associated with the ICE-6G ice history at 14.5 ka, during MWP-1a (see text for details).

67

68



69

70

71 Appendix Figure 4 | Grounding line position (relative to the initial position) calculated from the marine-terminating

72 glacier model using the GI-31 ice thickness and either the GI-31 (gray) or ICE-6G (blue) paleotopographies at 13 ka.

73 The dotted red line is the total grounding line retreat of the Amundsen Ice Stream reported by Lakeman et al. (2018).

